



US Army Corps
of Engineers®

Wave-Action Balance Equation Diffraction (WABED) Model: Tests of Wave Diffraction and Reflection at Inlets

by Lihwa Lin, Hajime Mase, Fumihiko Yamada, and Zeki Demirbilek

PURPOSE: Wave diffraction is a fundamental wave transformation process that occurs at all coastal inlets. The purpose of this Coastal and Hydraulics Engineering Technical Note (CHETN) is to demonstrate the numerical modeling capability to represent wave diffraction and reflection available in the WABED (Wave-Action Balance Equation with Diffraction) model. The WABED model is available as a nearshore wave transformation model in the Coastal Inlets Research Program's (CIRP's) Coastal Modeling System (CMS). Performance of the model is examined in this CHETN with two physical model data sets. The first data set pertains to a detached semi-infinite breakwater in front of a natural inlet, and an inlet with dual jetties. The second data set pertains to an inlet protected either by reflecting or absorbing jetties. Wave diffraction, wave reflection, and consequences of these processes on numerically simulated currents are examined with the two-dimensional (2-D) circulation model M2D. Future technical notes in this series will describe the interface and report additional validation and enhancements of WABED.

BACKGROUND: WABED is a 2-D wave spectral transformation (phased-averaged) model (Mase and Kitano 2000; Mase 2001; Mase et al. 2005). It is a phase-averaged model, which neglects changes in the wave phase in calculating wave and other nearshore processes from the output wave information. This class of wave models represents changes that occur only in the wave energy (action) density. Isobe (1998) and Panchang and Demirbilek (1998) have reviewed different types of wave prediction models for offshore and coastal engineering applications. Because phase-averaged energy (action) balance models neglect wave phase, they cannot directly predict wave diffraction and reflection caused by bathymetric features and structures. However, these effects may be incorporated in such models in approximate ways. For example, wave diffraction has been approximated in the STWAVE model as a form of diffusion (Smith et al. 1999), whereas wave reflection is omitted. Various methods have been investigated over the last 60 years to include diffraction and reflection in wave models (e.g., Penney and Price 1952; Rivero et al. 1997a, 1997b; Yu et al. 2000; and Holthuijsen et al. 2004).

The WABED model contains theoretically developed approximations for both wave diffraction and reflection and, therefore, is suitable for conducting wave simulations at coastal inlets. This CHETN presents results from an evaluation of the WABED capability for representation of diffraction and reflections at coastal inlets. Successful performance of WABED has resulted in its inclusion in CIRP's CMS. CIRP has improved model efficiency to minimize WABED run time, developed implementation of the model inside the Surface-water Modeling System (SMS), and added new capabilities to the model for calculation of wave radiation stresses for wave-induced current, and wave-generation-growth. WABED is implemented in the CMS through the

SMS, and input files are similar to those for the existing spectral model STWAVE (Smith et al. 1999) in the SMS.

WABED employs a forward-marching, finite-difference method to solve the wave action conservation equation. Capabilities of the WABED model include wave shoaling, refraction, diffraction, forward reflection, depth-limited breaking, dissipation, and wave-current interaction (Mase 2001; Mase et al. 2005). Wave diffraction is implemented by adding a diffraction term derived from the parabolic wave equation to the energy-balance equation. The model operates on a coastal half-plane so primary waves can propagate only from the seaward boundary toward shore. If the seaward reflection option is activated, the model will also perform backward marching for seaward reflection after the forwarding-marching calculation is completed.

The diffraction feature employed in WABED was originally tested for waves in a gap between two breakwaters as compared to the classical analytical Sommerfeld solution (Penney and Price 1952) for waves transforming on a uniform-depth bottom, and for waves transforming over a circular shoal in a laboratory experiment (Mase and Kitano 2000; Mase 2001; Mase et al. 2005). In this CHETN, the model is compared to measurements made in two CIRP physical model experiments for idealized inlet configurations on sloping beaches where waves refract, shoal, and break, in addition to diffract. The first experiment represented four types of inlets with a detached breakwater, a dogleg (or hook-shape) breakwater, a natural inlet, and a dual-jetty inlet (Seabergh et al. 2002). The second experiment had a dual-jetty inlet with absorbing or fully reflecting jetties (Seabergh et al. 2005). Comparisons of model results and measurements only for detached breakwater and dual-jetty inlet configurations of the first experimental study are presented in this CHETN to highlight modeling skill of WABED for wave diffraction and wave reflection at coastal inlet structures. For the second experiment, comparison of WABED with physical model data is presented for both absorbing and reflecting jetties of an idealized inlet.

Wave diffraction and reflection are often significant around coastal structures such as breakwaters and jetties. Because of these processes, wave transformation at inlets is generally complicated. Wave diffraction and other inlet processes can generate currents and modify the water level. Wave breaking in the surf zone near structures can also drive a current along the shore and structures. Wave and current interactions will further complicate the wave transformation around inlets. Therefore, it is necessary to include the possible interaction of the current in modifying wave properties at coastal inlets. In the WABED model, the effect of a current on waves is included as a Doppler shift in the solution of intrinsic frequency calculated through the wave dispersion equation. This treatment of the wave-current interaction is considered in other similar models (Smith et al. 1999; Lin and Demirbilek 2005). In this technical note, CIRP's 2-D circulation model M2D (Militello et al. 2004) is operated with WABED for calculation of the wave-induced current. A background flood current was supplied as input to the wave model. To calculate the wave-induced current, M2D was forced by radiation stresses (Longuet-Higgins and Stewart 1964) computed by WABED.

MODEL AND DATA COMPARISON WITH 2002 PHYSICAL MODEL: This physical model experiment was designed to collect wave data in the vicinity of an idealized inlet on a gentle sloping bottom (Figure 1). The experiment included four different structural configurations: a detached shore-parallel breakwater, a hook-shape breakwater, a natural inlet, and a

dual-jetty inlet (Seabergh et al. 2002; Lin and Demirbilek 2005). To consider wave diffraction and reflection, results of the numerical model and physical model measurements are compared here for the detached breakwater and dual-jetty inlet configurations. Table 1 lists the experiment conditions for the detached breakwater and dual-jetty inlet configurations. The detached breakwater configuration is denoted as Structure 1 (S1), and the dual-jetty inlet configuration as Structure 4 (S4). Both S1 and S4 were designed as fully reflecting structures in the experiment.

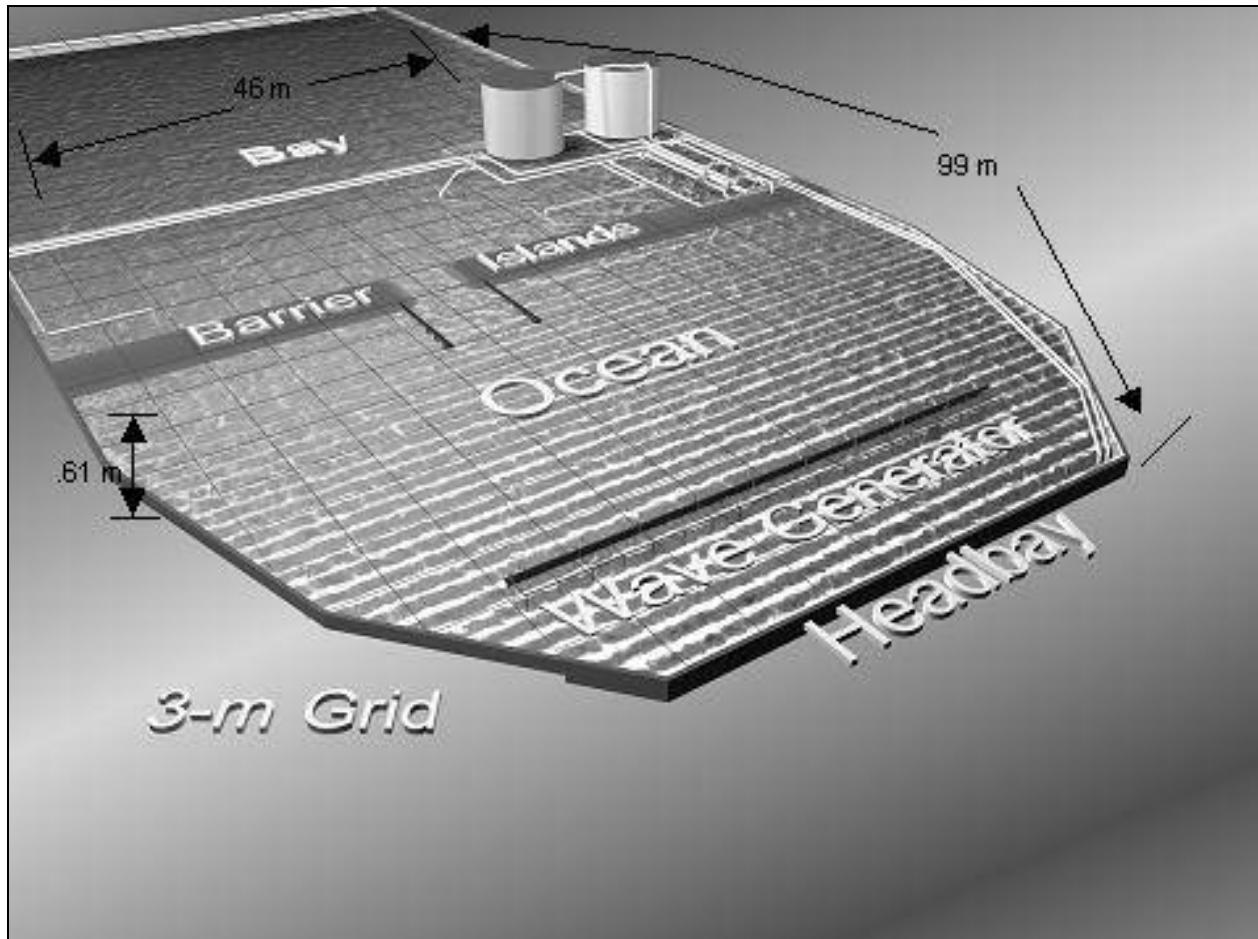


Figure 1. Idealized inlet model research facility.

Tested incident wave conditions include a regular (monochromatic) wave with a period of 5.7 sec and two JONSWAP-type irregular (spectral) unidirectional waves with peak period of 5.7 and 11.3 sec, representing both short and long period irregular waves. Froude scaling was applied to achieve prototype conditions for wave height and period. Incident wave angles were 20 and 0 deg, respectively, relative to shore-normal for S1 and S4. These incident wave conditions are labeled as X1 to X6 in the experiment. In addition, the test condition S4X5 had a constant flood current of 1 m/sec maximum velocity at the inlet throat (Froude scaled).

Table 1 Idealized Inlet Experimental Conditions (1:50 scale)					
Experiment Number	Wave Ht (m)	Wave Period (sec)	Wave Direction (deg)	Type	Current on/off
S1: Detached Breakwater (Offshore, Parallel to Shore)					
S1X4	3.05	5.7	20	Irregular	Off
S1X5	2.3	11.3	20	Irregular	Off
S1X6	2.3	5.7	20	Regular	Off
S4: Dual Jetties (Inlet and Bay Measurements)					
S4X1	3.05	5.7	0	Irregular	Off
S4X2	2.3	11.3	0	Irregular	Off
S4X3	2.3	5.7	0	Regular	Off
S4X5	2.3	11.3	0	Irregular	Flood
Note: Maximum steady flood current is 1 m/sec at the inlet. Various wave/current conditions are labeled as X1 to X6. Incident waves are unidirectional and direction is relative to shore-normal.					

In the physical model, wave height was measured by a linear array of capacitance wave gauges and wave direction by a remote-sensing video-camera system. The location of wave gauges and video-camera coverage area is shown in Figure 2. The accuracy of the wave height measurement is within 1 percent of full scale. The accuracy of wave direction measurement was calibrated by using the acoustic-Doppler velocimeters (ADV). Calibrated directional errors are calculated as 4.6 and 7.7 deg for S1 and S4, respectively. For S1, wave height and direction measurements were made in the lee side (shoreward) of the breakwater. For S4, wave data were collected between jetties and in the bay area. For further information, see Lin and Demirbilek (2005) and Seabergh et al. (2002).

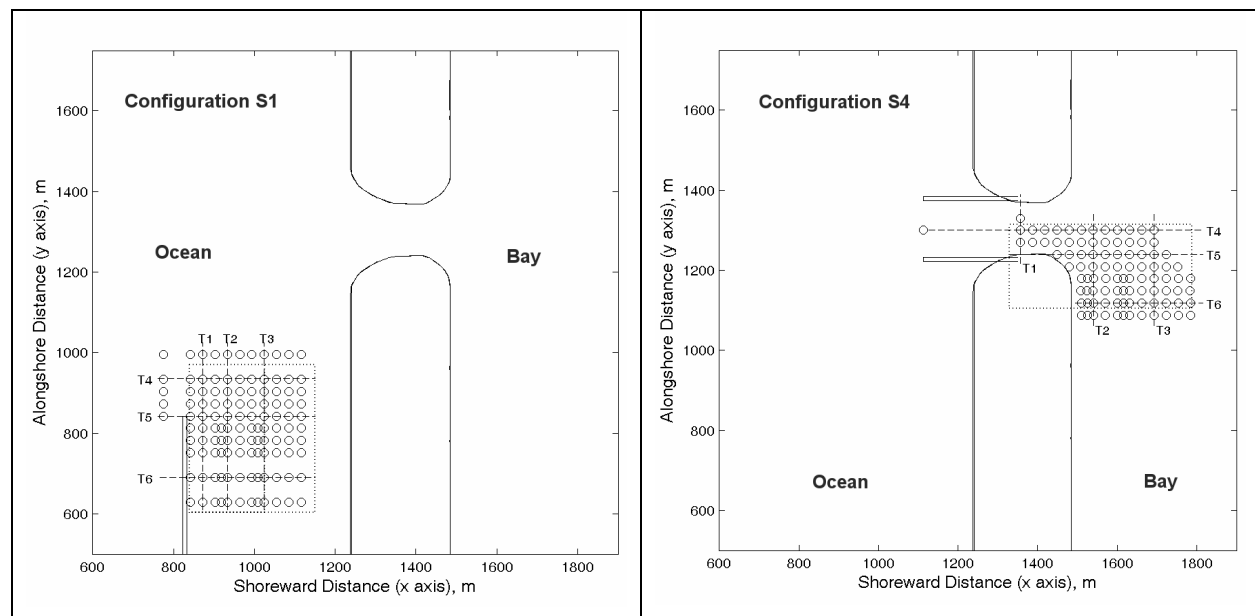


Figure 2. Location map of wave gauges (circle), rectangular area covered by video-camera system (dotted line), and transect lines (dashed line) for wave model and data comparisons.

For each physical model test condition, three WABED simulations were performed: (a) non-reflecting (fully absorbing) jetty with a zero reflection coefficient R in the model, (b) fully reflecting jetty ($R = 1$), and (c) coupled wave-circulation model simulation with $R = 1$ and wave-current interactions. The dimension of the numerical grid is 1,600 m in the shore-normal direction (x-axis) and 1,800 m in the alongshore direction (y-axis). The same grid was used in both wave and circulation models. The origin of the grid is located at $x = 450$ m and $y = 300$ m. The size of each grid cell is 10 m by 10 m. The inlet is approximately located in the center of the grid. For each of these simulations, WABED results vs. measurements are presented along six transects (Figure 2). The comparison for the detached breakwater case is emphasized in the diffracted wave area in the lee of the breakwater. For the jettied inlet case, the comparison is emphasized in the inlet channel and in the diffracted wave area in the bay.

For S1, there was no significant difference between predicted wave height and direction and measurements in the lee (shoreward) of the detached breakwater. Typically, wave diffraction was strong in the lee of a detached breakwater, and wave reflection was negligible. The effect of wave-induced currents and wave-current interactions on wave diffraction in the lee of this detached breakwater was insignificant because the current was weak in the diffraction region behind the breakwater.

Figures 3 and 4 provide a comparison of model predicted wave height and direction (with $R = 1$ in the wave model simulation) and data along six transects for two irregular incident wave conditions S1X4 and S1X5. Three statistical parameters are calculated (Table 2) as a measure of agreement between model calculations and measurements. The first is the mean of the absolute relative error for wave height, defined as the percent change of calculated wave height and data (i.e., $100 \text{ percent} \times |\text{predicted-measured}|/\text{measured}$). The second is the mean of the absolute difference (bias) for wave height. The third is the mean of the absolute difference of calculated and measured wave direction (Lin and Demirbilek 2005). Wave period was not considered in the comparison because the peak period did not change in either the physical model or the numerical model. The statistics presented for S1 in Table 2 are averaged values of all alongshore and cross-shore transects in each test condition. Among three S1 experimental conditions, the wave height estimate of the short irregular wave has the smallest error (23.3 percent for the mean absolute relative error and 0.2 m for the mean absolute bias). The mean error of the wave direction estimate is similar for three experimental conditions, varying from 7.2 to 7.7 deg. Agreement between predicted wave directions and data along all transects is not as good as compared to wave height. Wave heights have the highest difference at transect T5, whereas noticeable deviation is seen along all transects between predicted wave directions and data.

For the dual-jetty inlet configuration (S4), the difference between three WABED results ($R = 0$, $R = 1$, and $R = 1$ coupled with the circulation model M2D) is more notable. For coupling, the wave field was calculated initially without current field and updated at 3-hr intervals after the current field was calculated between two consecutive wave field estimates. Wave radiation stresses are used to force the circulation model. The coupling of wave and circulation models was made for a total of 6-hr simulation in this study. For S4X5, a flood current is simulated in the circulation model by specifying the water level gradient between the seaward and bayward boundaries. Similar statistics to those in S1 are calculated in wave height and direction for S4.

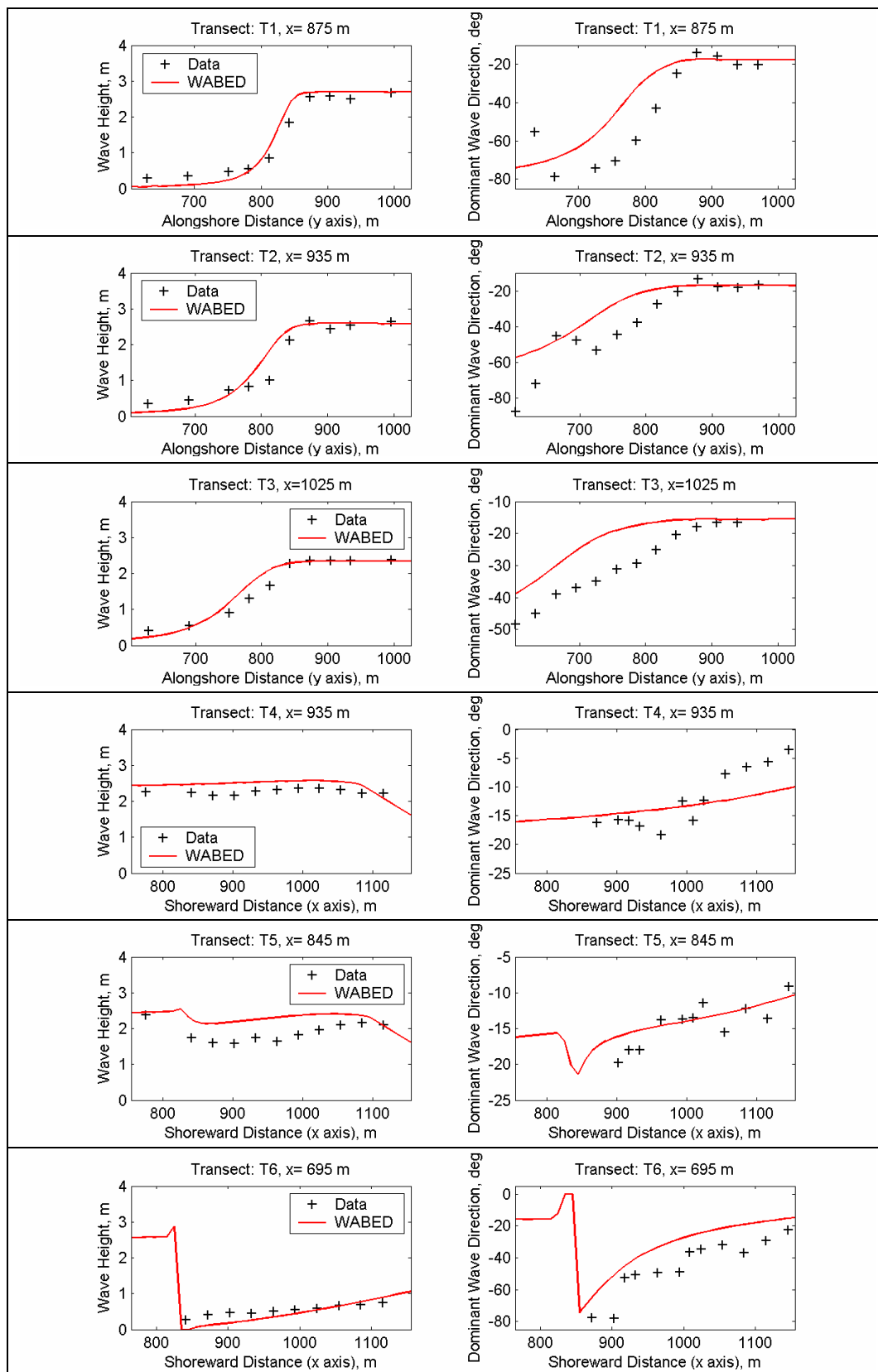


Figure 3. Calculated versus measured wave height and direction for S1X4 (R=1).

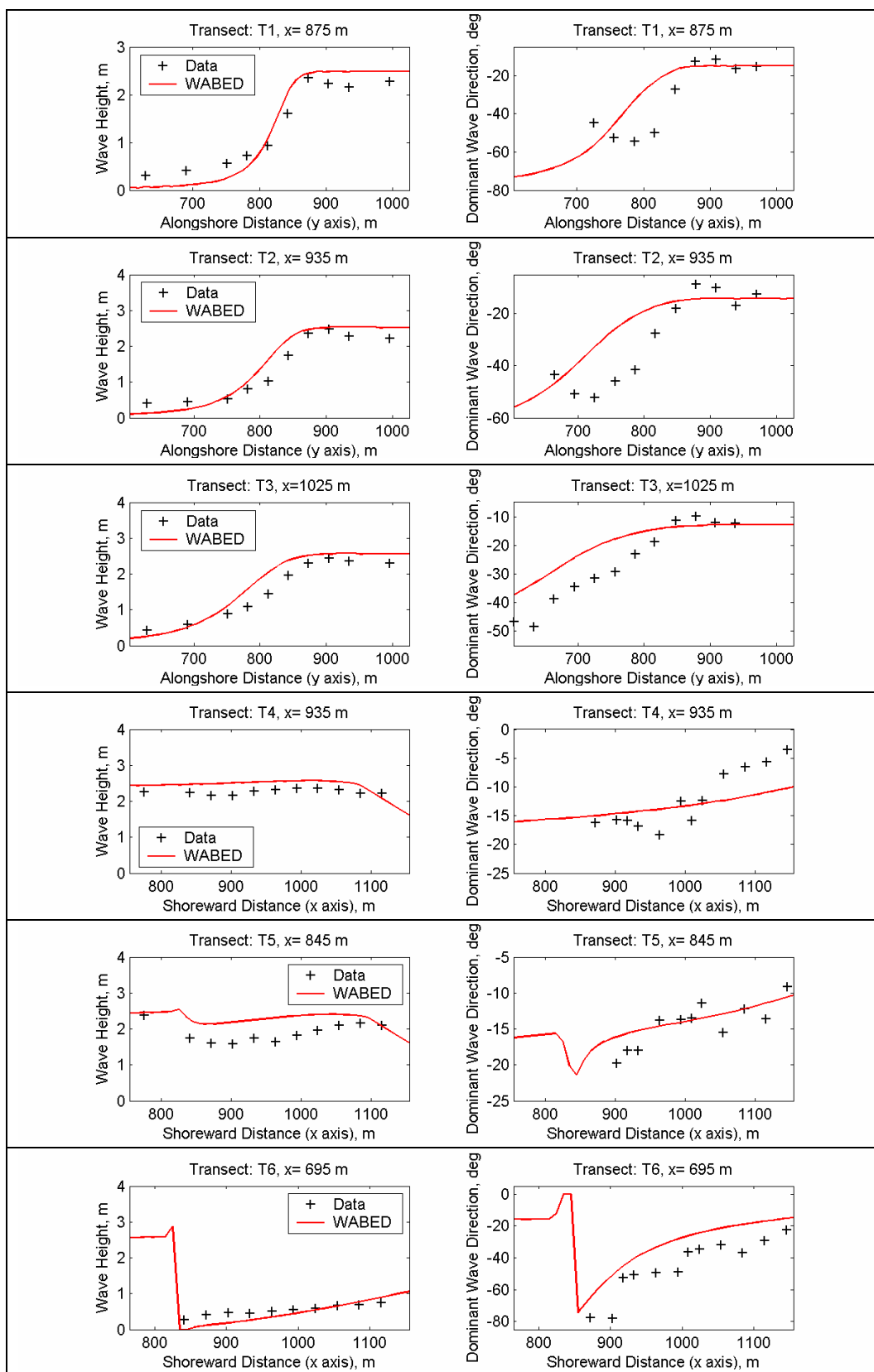


Figure 4. Calculated versus measured wave height and direction for S1X5 (R=1).

Table 2 Statistical Mean Errors of Calculated Height and Direction for Configuration S1			
Experiment Number	Mean of Absolute Relative Wave Height Error (%)	Mean of Absolute Wave Height Error (m)	Mean of Absolute Wave Direction Error (deg)
S1X4	23.3	0.20	7.7
S1X5	25.8	0.27	7.2
S1X6	28.4	0.21	7.6
Average	25.8	0.23	7.5

Figure 5 compares both wave height and direction with data along six transects for S4X1 corresponding to a fully reflecting jetty ($R = 1$) and coupled wave-circulation models. Figure 6 compares wave height and direction for S4X3 with absorbing ($R = 0$) and fully reflecting ($R = 1$) jetties. Figure 7 provides comparison of calculated wave height and direction with data for S4X5 corresponding to the reflecting jetty ($R = 1$) and coupled wave-circulation models. These calculated wave heights agree well with data at the inlet (Transect 1). The agreement improves with the coupled simulation compared to a wave model alone case. Such good agreement between model and data at the inlet ensures reliability of wave estimates in the bay area. Table 3 provides the calculated statistics for four test conditions used in S4. These statistics indicate the WABED model predicts reliable wave height estimates with $R = 1$ for a fully reflecting jetty. The wave direction estimates obtained for the shorter irregular wave (S4X1) have the smallest mean error of 3.6 deg with values of $R = 0$ and $R = 1$. This error for a coupled simulation of WABED-M2D is 3.7 deg. Overall, the calculated errors for S4 in wave height and direction for tested wave conditions are slightly less than the resulting errors for S1.

MODEL AND DATA COMPARISON WITH 2005 PHYSICAL MODEL STUDY: The second laboratory experiment was designed to collect both current and wave data in the vicinity of an idealized dual-jetty inlet that was similar to configuration S4 in the first (2002) experiment. Two different jetty types, absorbing and reflecting, were constructed, and tests were performed with three incident regular (monochromatic) wave conditions. These included a short wave of small wave height (X6), a long wave with moderate wave height (X7), and a short wave with large wave height, X8 (Seabergh et al. 2005). For convenience, the fully absorbing jetty inlet is denoted here as Configuration S5, and the fully reflecting jetty inlet as S6. Only moderate long wave (X7) and large short wave (X8) were simulated by WABED for evaluation of wave diffraction and reflection associated with two types of jetties. Tested incident waves were unidirectional and 20 deg oblique to shore normal. Table 4 lists the incident wave conditions. This experiment did not include a flood or ebb current at the inlet.

Both wave and current were measured on the up-wave side of the south jetty in the S5 and S6 configurations. Additional wave and current data were collected inside the inlet (between dual jetties) for S5. Wave height was measured from a linear array of capacitance wave gauges as was done in the first laboratory experiment. Currents were collected from a linear array of ADV instruments, and wave direction was calculated from the current vector data using a standard stochastic method (Cartwright 1963). Figure 8 shows the location of these linear arrays of wave gauges and ADV instruments.

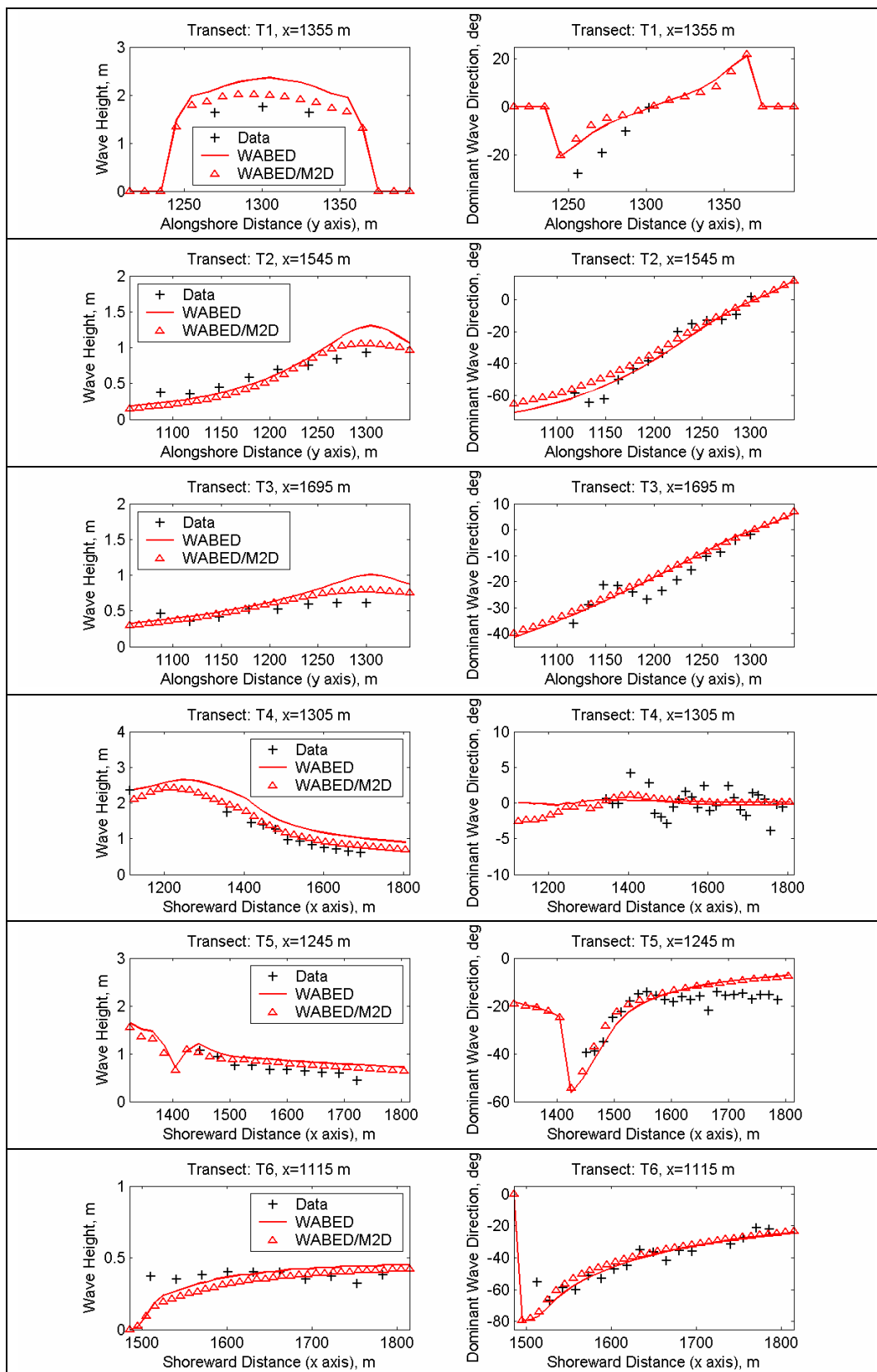


Figure 5. Calculated versus measured wave height and direction for S4X1 (R=1).

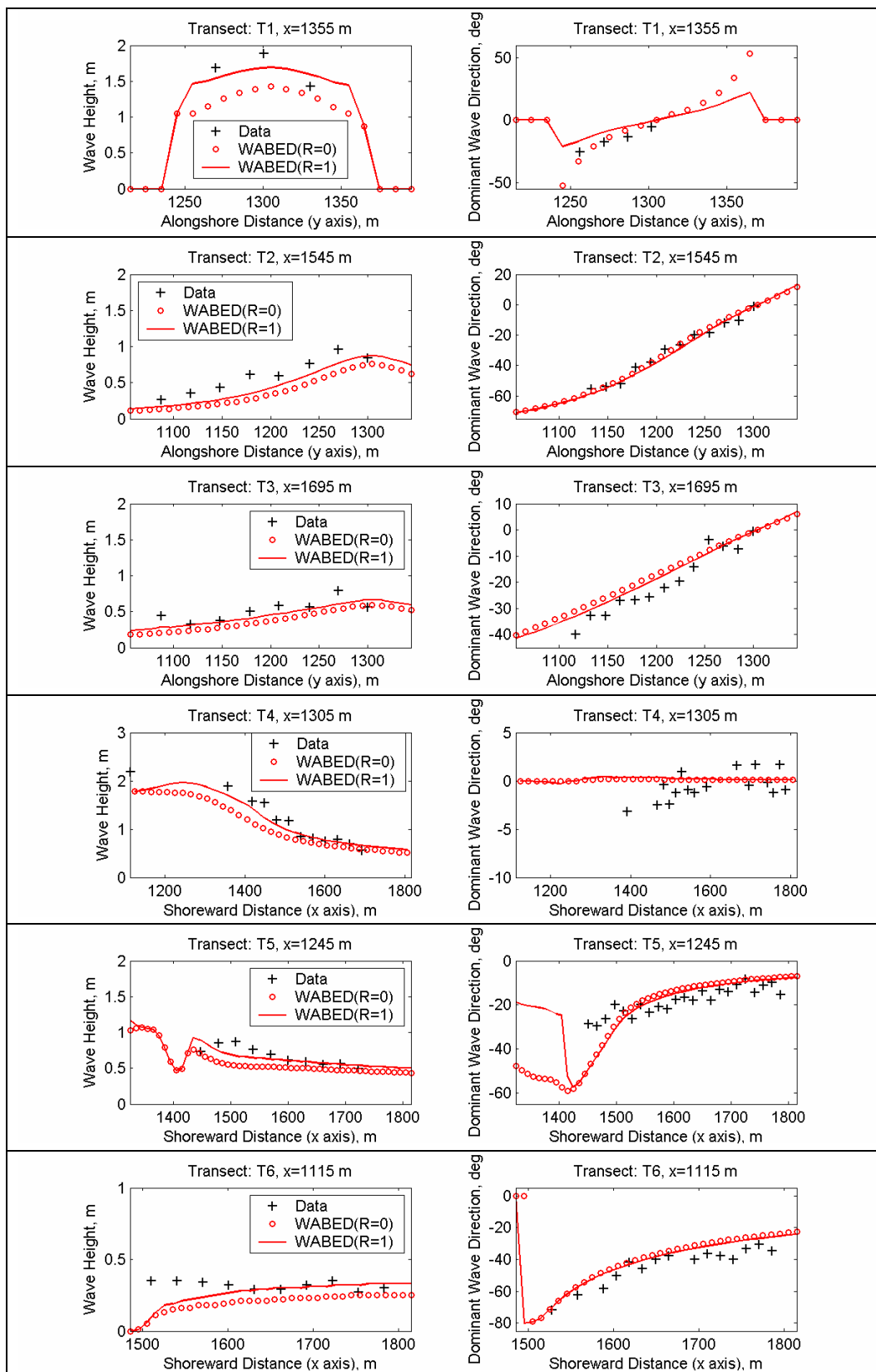


Figure 6. Calculated versus measured wave height and direction for S4X3 (R=0 & R=1).

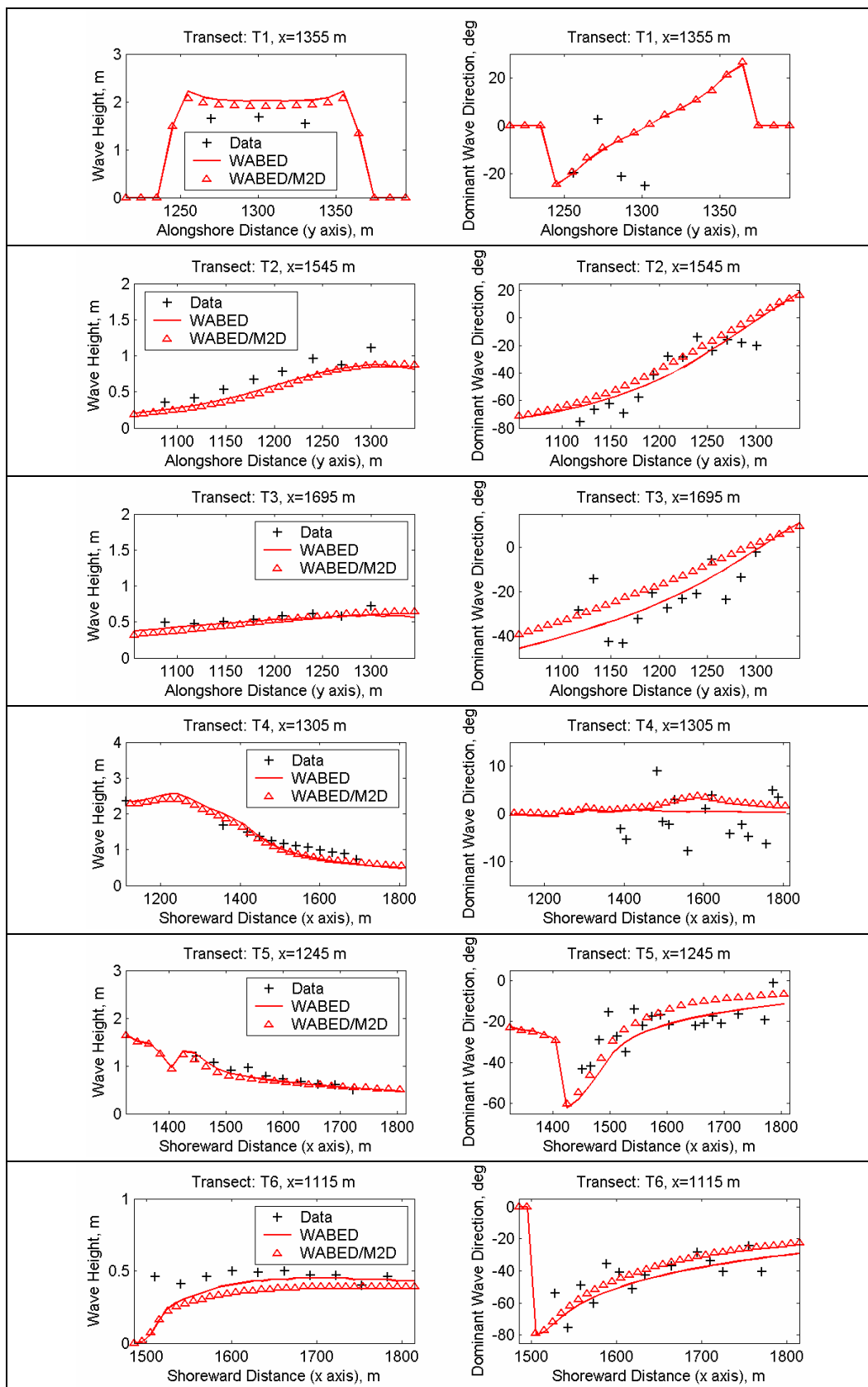


Figure 7. Calculated versus measured wave height and direction for S4X5 (R=1).

Table 3
Statistical Mean errors of Calculated Height and Direction for Configuration S4

Experiment Number	Mean of Absolute Relative Wave Height Error (%)	Mean of Absolute Wave Height Error (m)	Mean of Absolute Wave Direction Error (deg)
Simulation with $R = 0$ for Jetties			
S4X1	23.8	0.15	3.6
S4X2	29.0	0.20	7.6
S4X3	28.0	0.19	4.7
S4X5	41.2	0.31	7.8
Average	30.5	0.21	5.9
Simulation with $R = 1$ for Jetties			
S4X1	31.0	0.23	3.6
S4X2	17.0	0.14	7.8
S4X3	15.9	0.07	4.3
S4X5	16.1	0.13	7.6
Average	20.0	0.14	5.8
Simulation with $R = 1$ and Coupling with M2D			
S4X1	20.2	0.13	3.7
S4X2	19.8	0.14	7.5
S4X3	23.5	0.16	4.9
S4X5	19.2	0.14	8.4
Average	20.7	0.14	6.1

Table 4
Fully Absorbing and Reflecting Jetty Experimental Condition (1:50 Scale)

Experiment Number	Wave Ht (m)	Wave Period (sec)	Wave Direction (deg)	Type	Current on/off
S5: Fully Absorbing Jetty					
S5X7	2.0	11	-20	Regular	Off
S5X8	3.4	8	-20	Regular	Off
S6: Fully Reflecting Jetty					
S6X7	2.0	11	-20	Regular	Off
S6X8	3.4	8	-20	Regular	Off

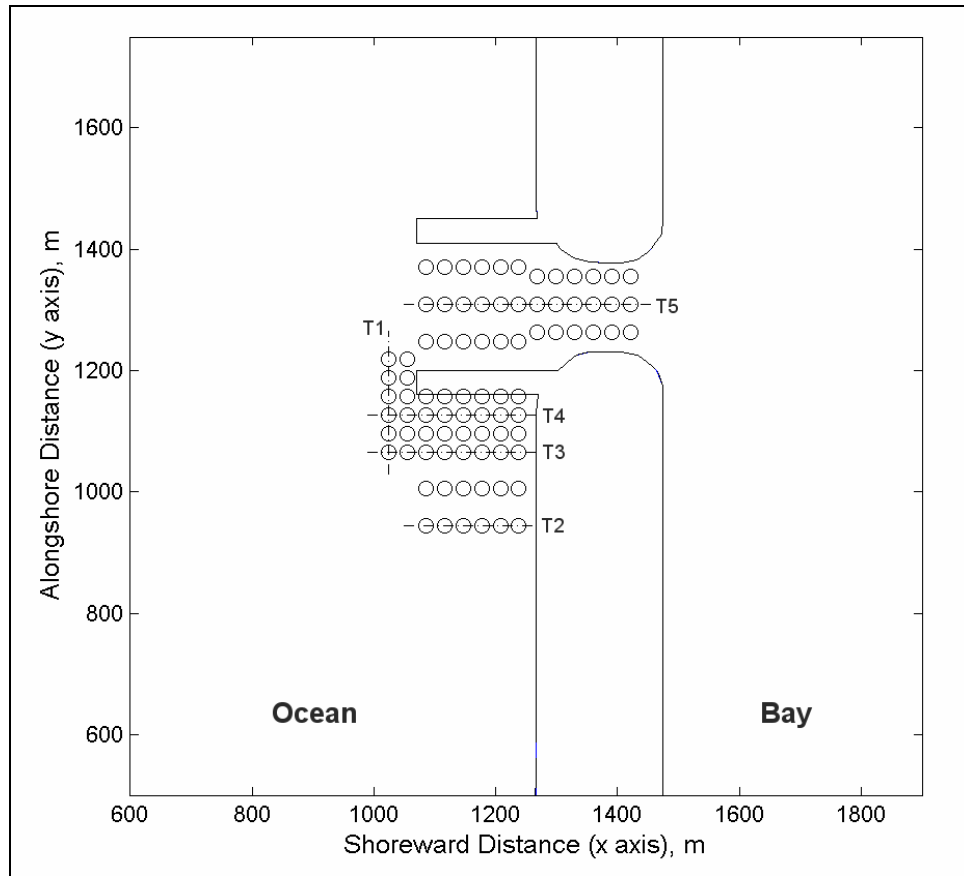


Figure 8. Location map of wave and current measurement stations (circle) and transect lines (dashed line) for wave model and data comparisons – Configurations S5 and S6.

The numerical simulations for S5 were coupled runs of WABED-M2D made with $R = 0$ in the wave model (perfectly absorbing jetty). The two models were coupled at a 3-hr interval for a total of a 6-hr simulation. For S6, a coupled simulation with $R = 1$ was made to represent a fully reflecting jetty. Figures 9 to 12 show calculated and measured wave fields for the four experiments S5X7, S5X8, S6X7, and S6X8, respectively. The calculated wave height and direction are shown in these figures as vector quantities and wave height also shown in black contours. Measured wave height and direction data are depicted in red vectors and blue contours. For absorbing the jetty, the good agreement between model and data is obtained in the inlet channel. In the area outside the inlet (south side of the south jetty), model and data are in good agreement near the shore, but differences between wave-height contours appear starting around one-half length of the jetty. The largest difference occurs for reflecting jetty with the incident wave condition X7.

Figures 13 to 16 compare calculated and measured wave height and direction along five and four transects for S5 and S6, respectively, corresponding to incident wave conditions X7 and X8. Table 5 lists the calculated mean statistical errors between numerical estimates and data collected along transects T1 to T5 located south of the up-wave jetty and inlet area (see Figure 8). These

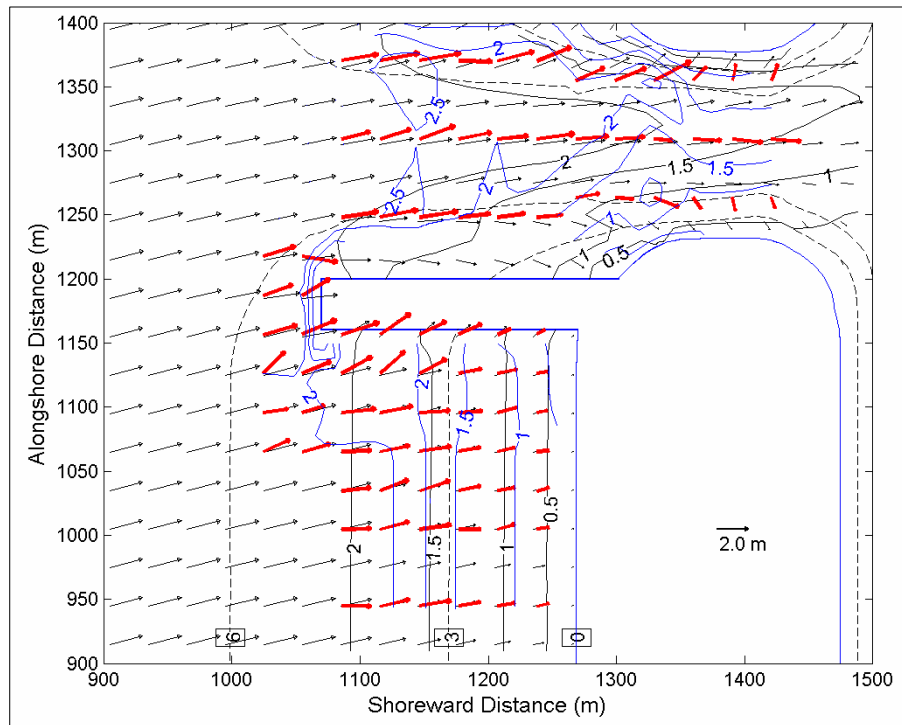


Figure 9. Calculated (WABED and M2D) versus measured wave fields for S5X7 (measured wave shown in red vectors and blue contours; depth contours indicated by dashed lines).

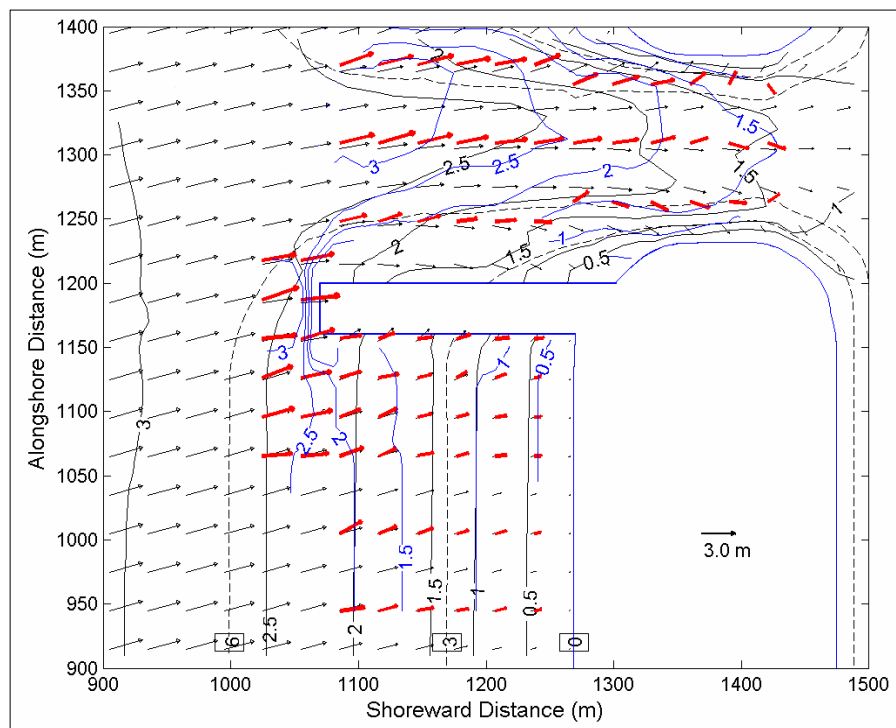


Figure 10. Calculated (WABED and M2D) versus measured wave fields for S5X8 (measured wave shown in red vectors and blue contours; depth contours indicated by dashed lines).

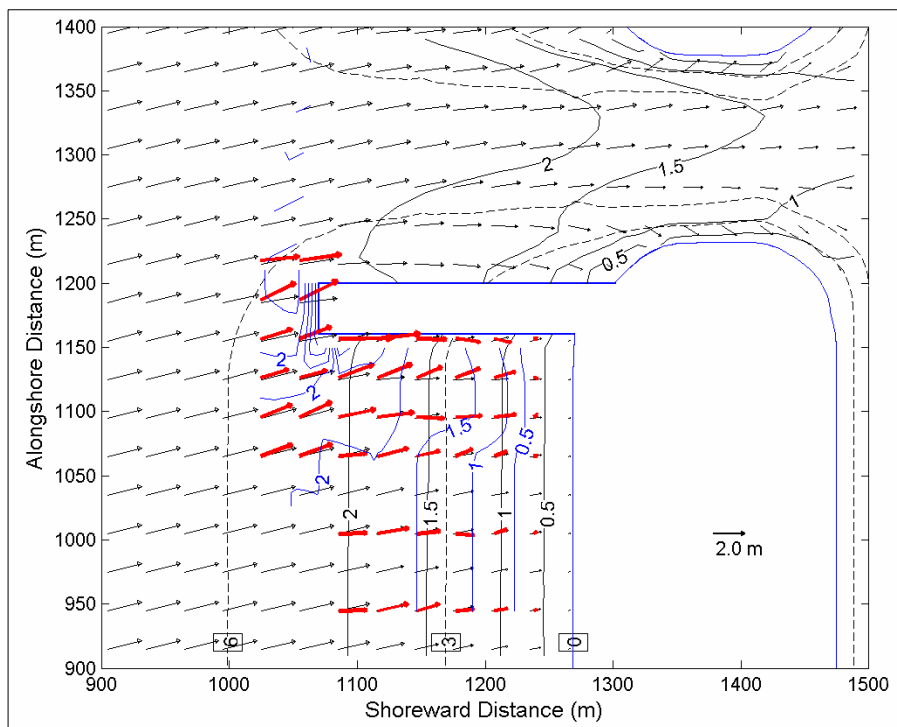


Figure 11. Calculated (WABED and M2D) versus measured wave fields for S6X7 (measured wave shown in red vectors and blue contours; depth contours indicated by dashed lines).

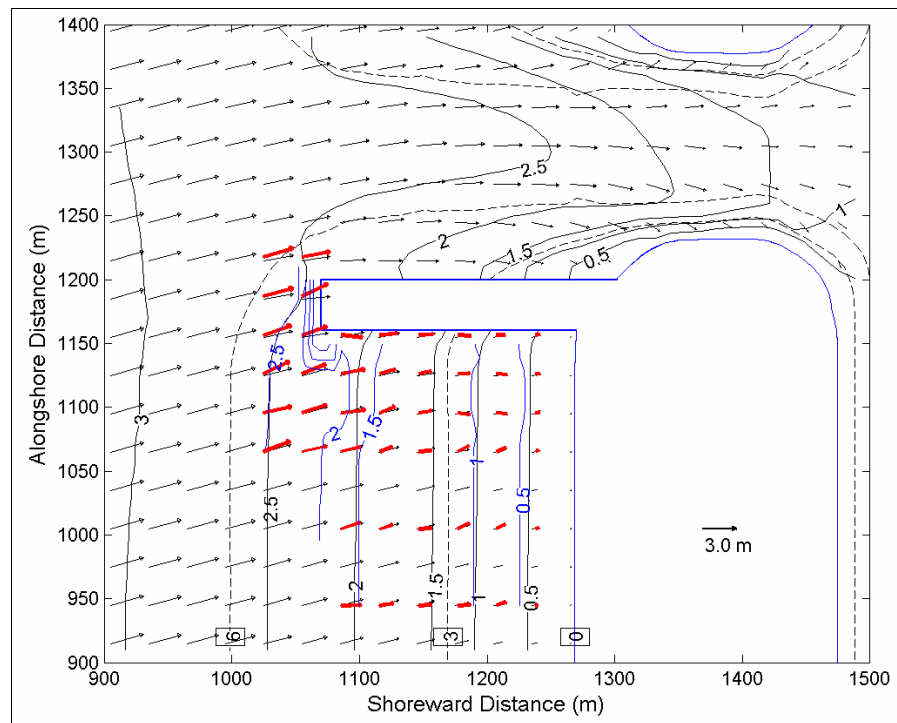


Figure 12. Calculated (WABED/M2D) versus measured wave fields for S6X8 (measured current shown in red vectors and blue contours; depth contours indicated by dashed lines).

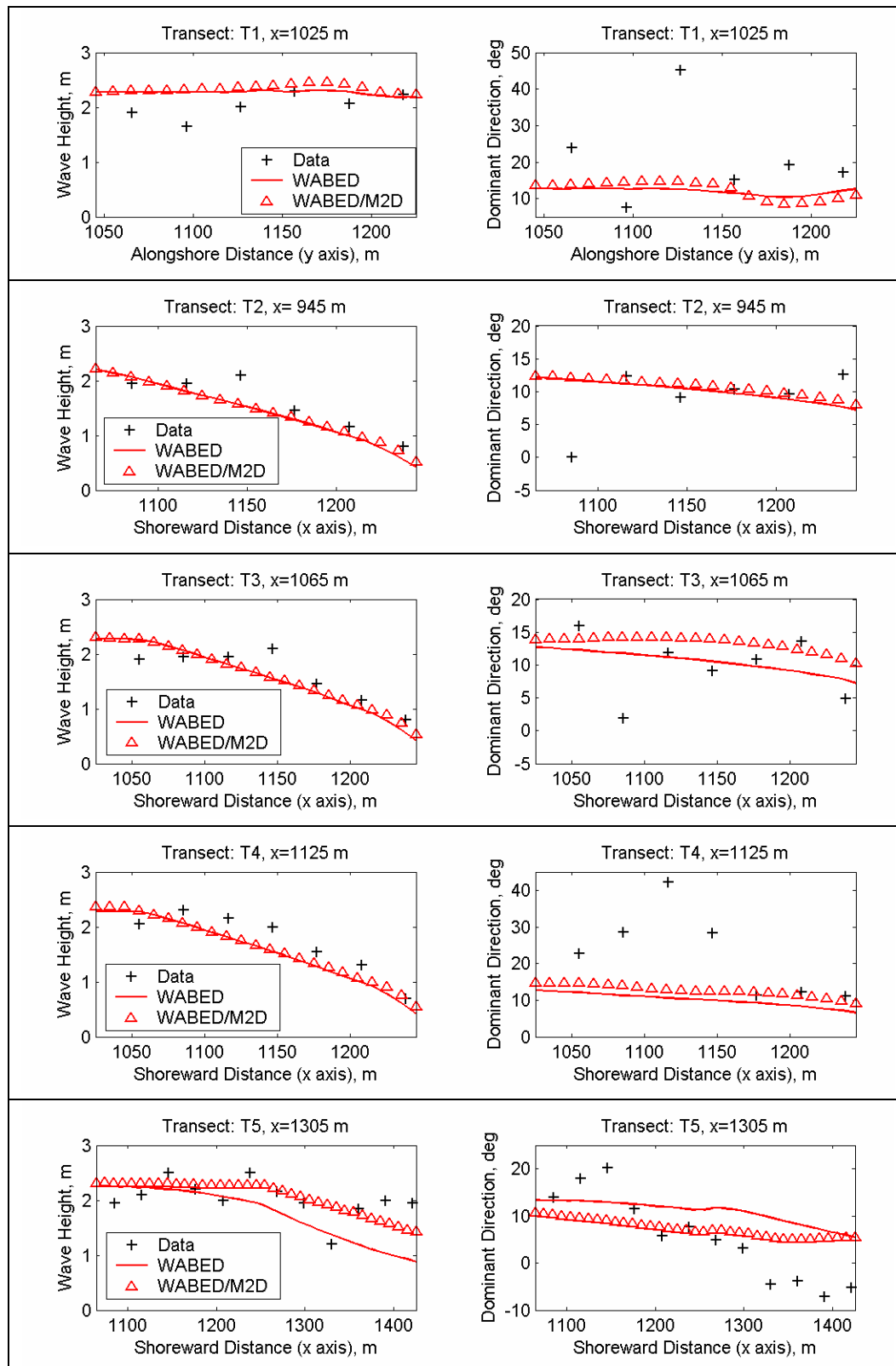


Figure 13. Calculated versus measured wave height and direction for S5X7.

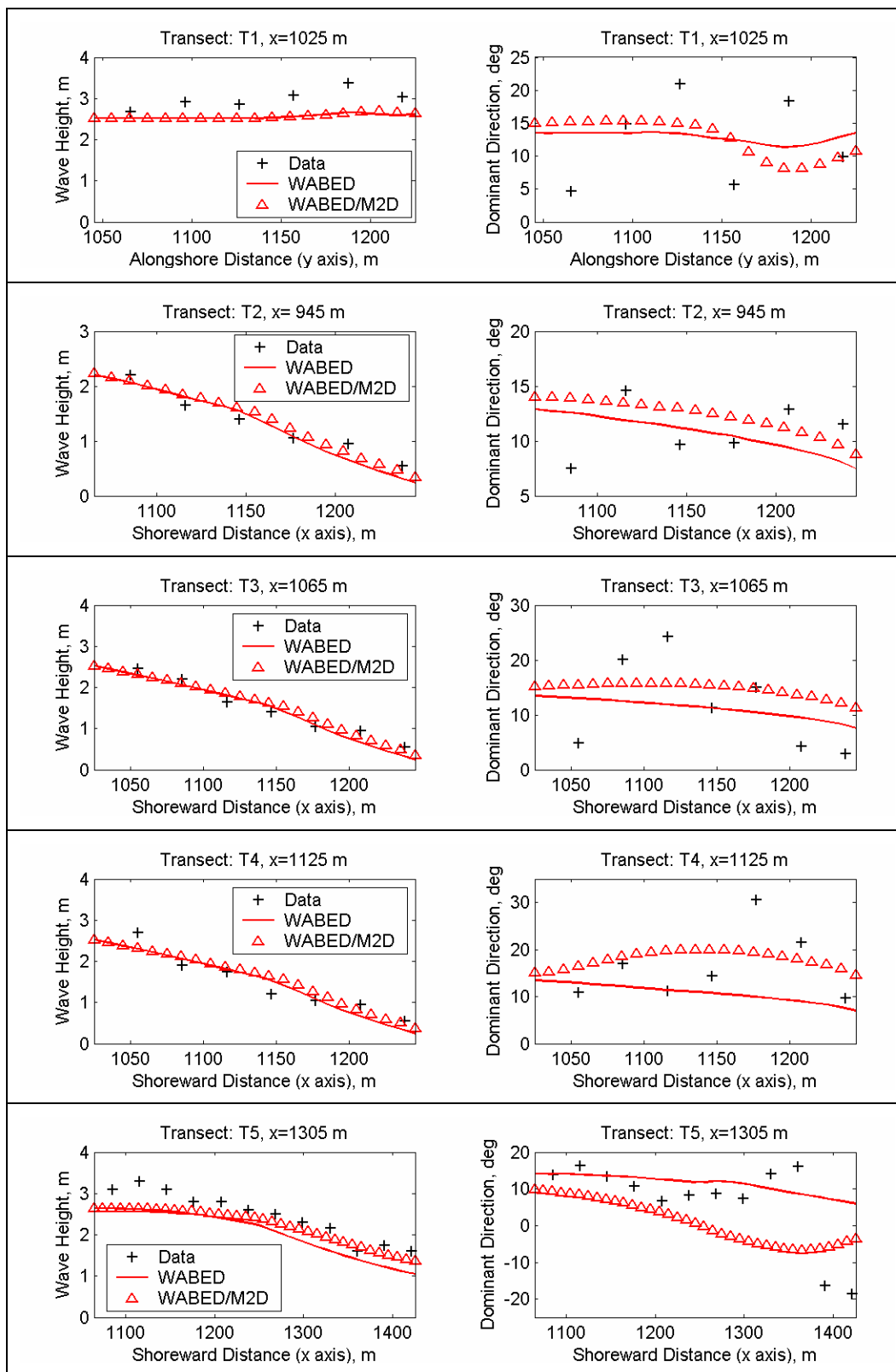


Figure 14. Calculated versus measured wave height and direction for S5X8.

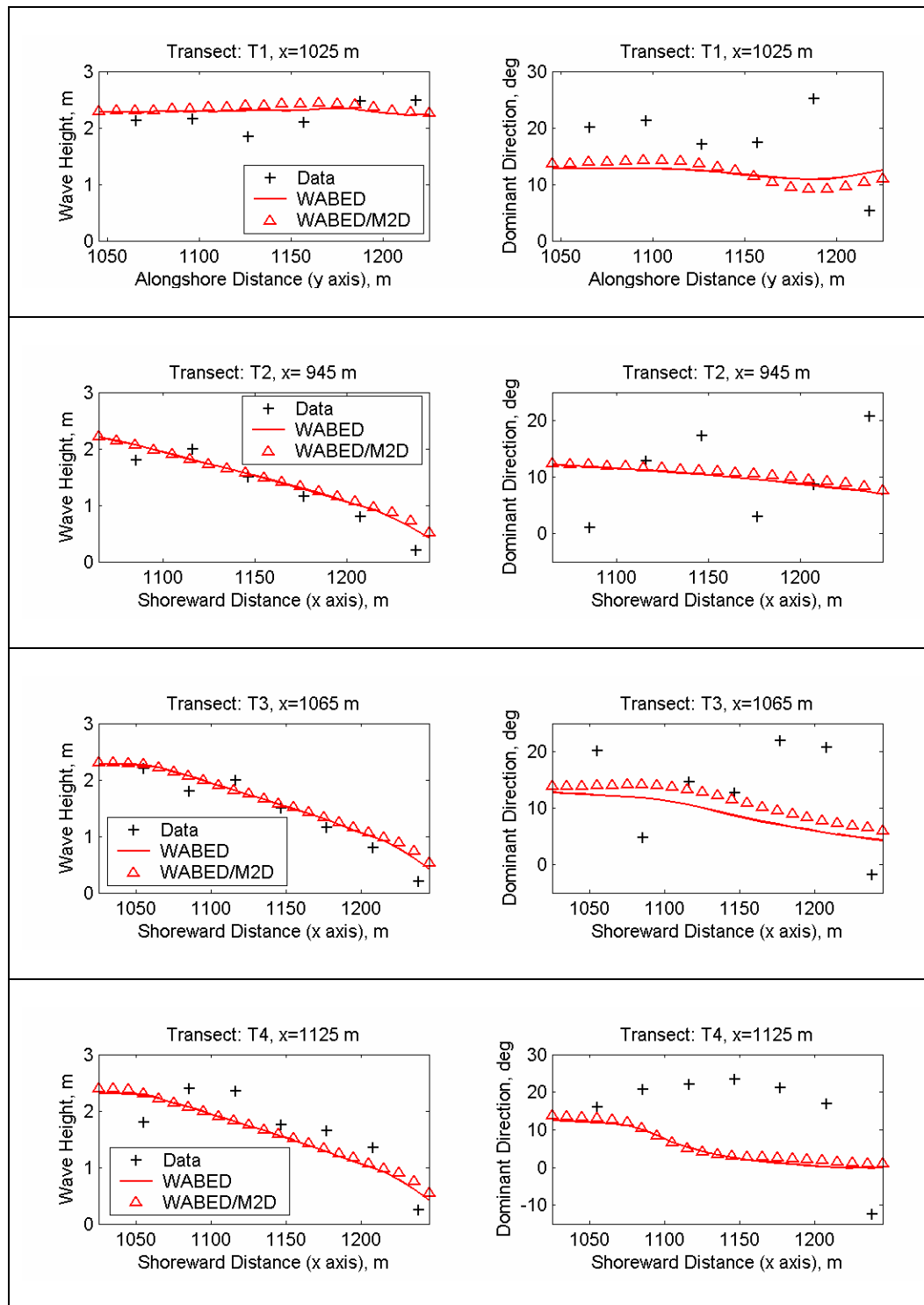


Figure 15. Calculated versus measured wave height and direction for S6X7.

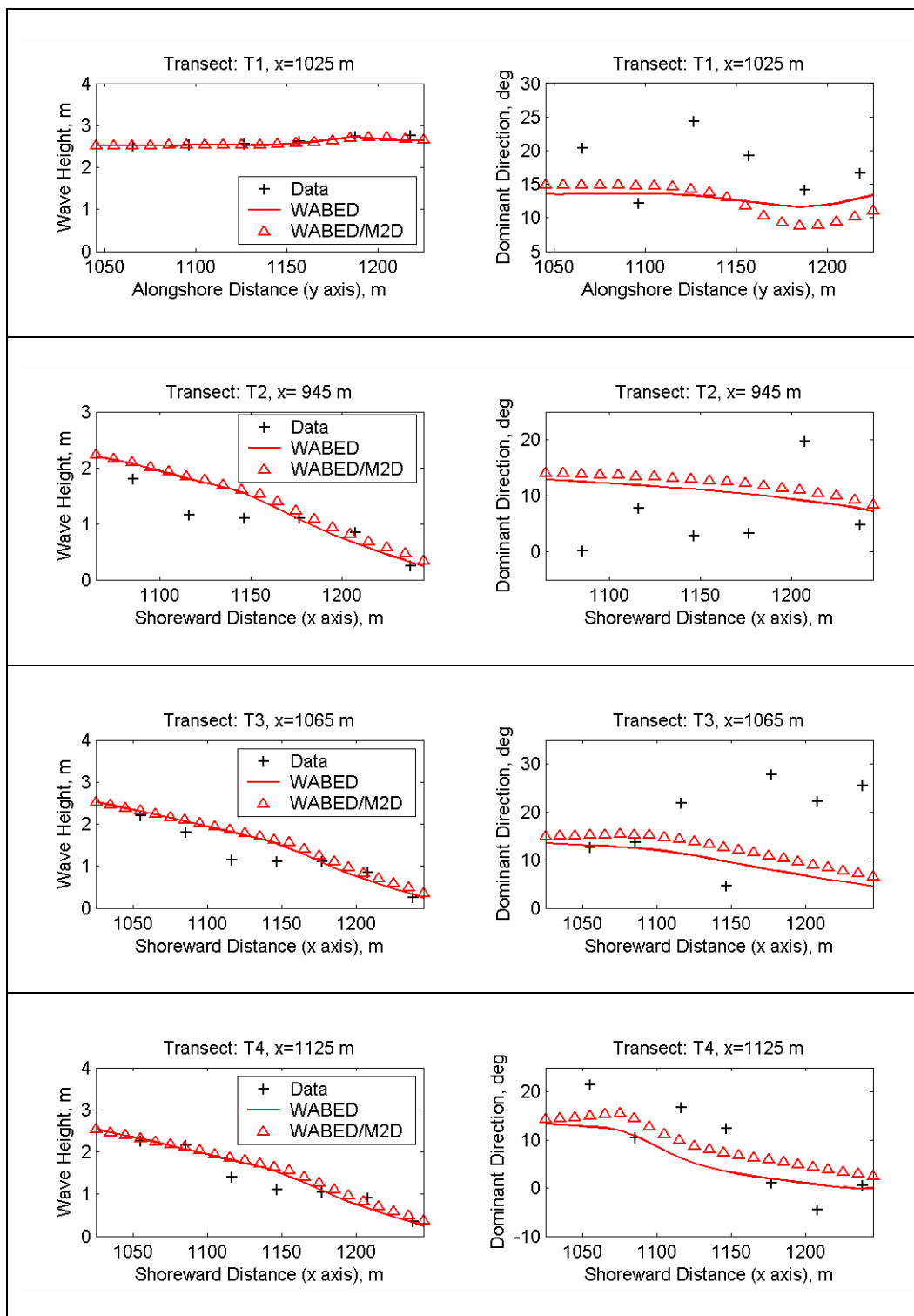


Figure 16. Calculated versus measured wave height and directions for S6X8.

Table 5 Statistical Mean Errors of Calculated Height and Direction for Configurations S5 and S6			
Experiment Number	Mean of Absolute Relative Wave Height Error (%)	Mean of Absolute Wave Height Error (m)	Mean of Absolute Wave Direction Error (deg)
Simulation by WABED			
S5X7	16.6	0.30	7.6
S5X8	19.9	0.30	5.9
S6X7	33.9	0.25	9.5
S6X8	18.0	0.19	7.2
Average	22.1	0.26	7.6
Simulation by WABED and M2D			
S5X7	13.9	0.24	7.0
S5X8	13.1	0.25	6.9
S6X7	41.4	0.28	9.0
S6X8	24.3	0.22	7.5
Average	23.2	0.25	7.6
NOTE: For coupling WABED and M2D, the two models were run alternatively in the 3-hr interval for a total of a 6-hr simulation.			

statistics errors of wave height and direction estimates are calculated for using WABED alone and coupled WABED-M2D simulations. It is evidenced that both WABED alone and coupled WABED-M2D predict well wave fields in the inlet area for both absorbing and fully reflecting jetties. The coupled WABED-M2D can calculate the circulation field influenced and induced by waves. Figures 17 to 20 show calculated wave-induced current fields (black vector) and measured currents (red vector) for S5 and S6 under incident wave conditions X7 and X8. The calculated current generally agrees well with the measured data in magnitude, direction, and current pattern in the up-wave jetty south and inlet area. At the center line of the inlet channel, the coupled WABED-M2D predicts a return current (from bay to ocean) that is shown in the data. However, the WABED-M2D does not predict the circulation cell developed in the up-wave area of the reflecting jetty. This will be investigated in the future study.

CONCLUSION: This CHETN introduces the wave spectral transformation model WABED for operations within the SMS and coupling with the M2D model for coastal inlet and nearshore applications depending particularly on calculation of wave diffraction. WABED represents and emphasizes both wave diffraction and wave reflection processes that significantly alter wave transformation at coastal inlets, in particular, those stabilized with jetties. Validation results for WABED model with two sets of laboratory data are presented. Model predictions compare well with data for four types of inlets structures over a wide range of wave and current conditions that have been evaluated here. Results of this systematic study have shown clearly that WABED is capable of describing wave diffraction and reflection at detached shore-parallel breakwaters and around both absorbing and reflecting jetties.

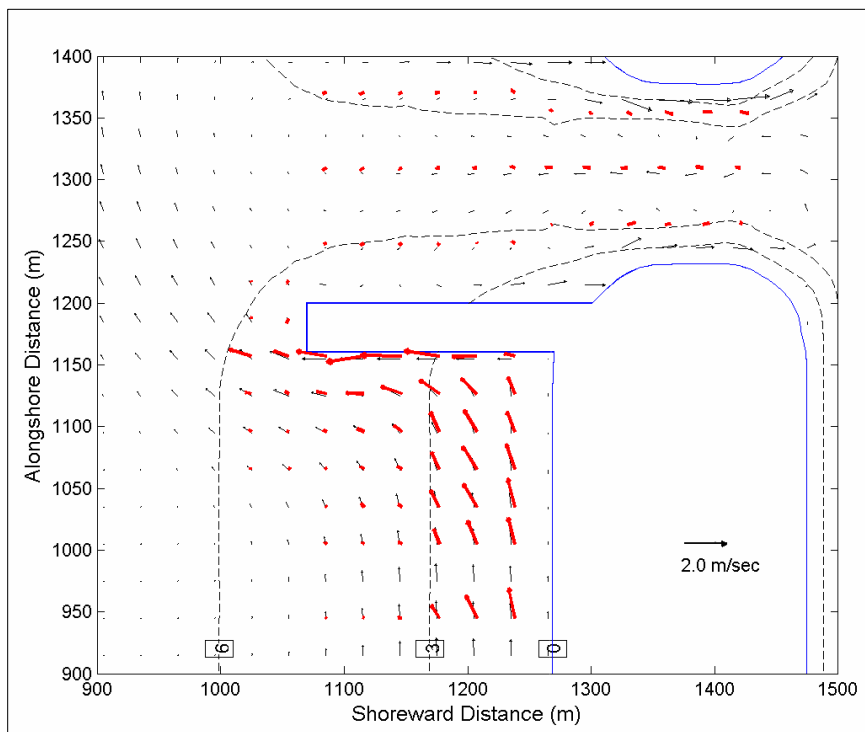


Figure 17. Calculated (WABED and M2D) versus measured current fields for S5X7 (measured current shown in red vectors; depth contours indicated by dashed lines).

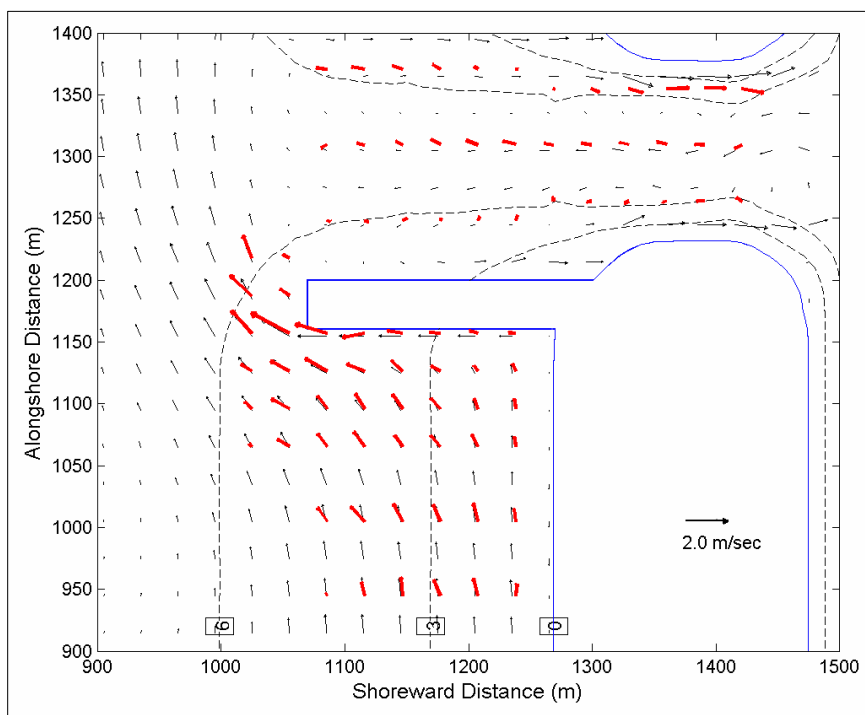


Figure 18. Calculated (WABED and M2D) versus measured current fields for S5X8 (measured current shown in red vectors; depth contours indicated by dashed lines).

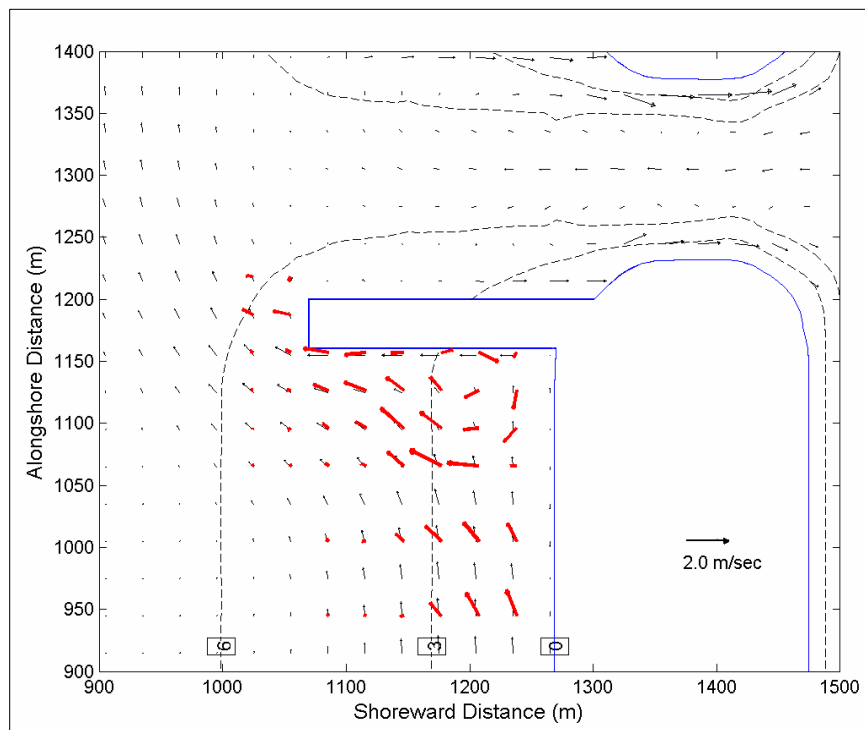


Figure 19. Calculated (WABED and M2D) versus measured current fields for S6X7 (measured current shown in red vectors; depth contours indicated by dashed lines).

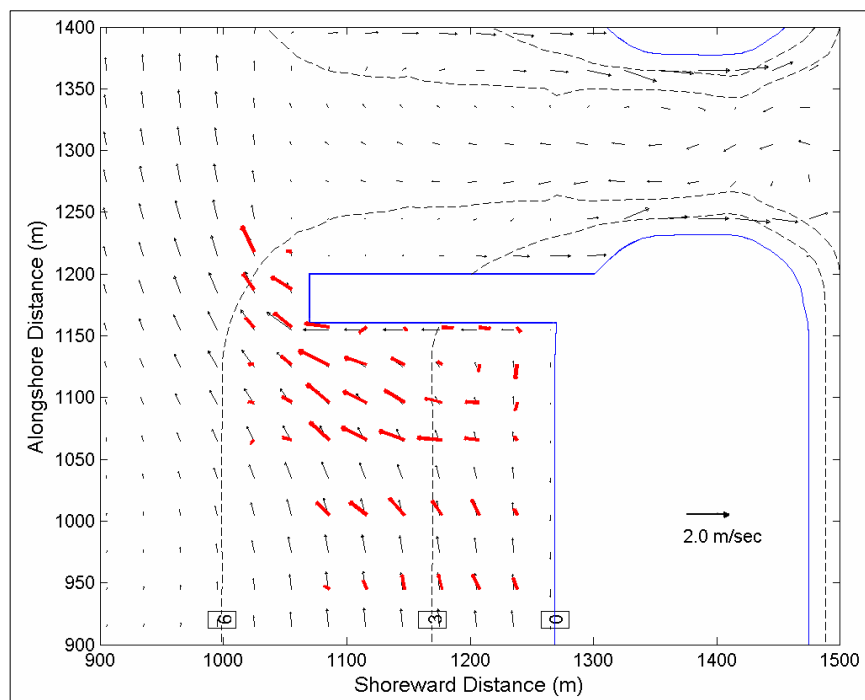


Figure 20. Calculated (WABED and M2D) versus measured current fields for S6X8 (measured current shown in red vectors; depth contours indicated by dashed lines).

The WABED model can be coupled to a 2-D circulation model (M2D) to calculate wave-induced currents resulting from wave breaking and wave-current interactions at coasts. Results from the coupled simulations demonstrate the capability of the WABED to provide correct wave forcing to circulation model at an idealized inlet. In general, the coupled WABED-M2D predicts well both wave and current fields with regular and irregular incident waves of short and long periods. Future studies will address comparison of model to field data and investigation of the grid nesting and wave-generation-growth capabilities of WABED. Wave generation and growth by wind has been added to WABED, and this feature will be described in a separate technical note in the WABED series.

POINTS OF CONTACT: This CHETN was written by Dr. Lihwa Lin, U.S. Army Engineer Research and Development Center, Coastal and Hydraulics Laboratory, 3909 Halls Ferry Road, Vicksburg, MS, 39180, Tel: 601-634-2704, Fax: 601-634-3088; Dr. Hajime Mase (mase@kaigan.dpri.kyoto-u.ac.jp) of the Kyoto University, Japan, Dr. Fumihiko Yamada (yamada@kumamoto-u.ac.jp) of Kumamoto University, Japan, and Dr. Zeki Demirbilek (Zeki.Demirbilek@usace.army.mil) of the U.S. Army Engineer Research and Development Center (ERDC), Coastal and Hydraulics Laboratory. Questions about this CHETN can be addressed to Lihwa.Lin@erdc.usace.army.mil. Inquiries about the Coastal Inlets Research Program can be directed to the Program Manager, Dr. Julie Rosati, Julie.D.Rosati@usace.army.mil. This technical note should be referenced as follows:

Lin, L., H. Mase, F. Yamada, and Z. Demirbilek. 2006. *Wave-action balance diffraction (WABED) model tests of wave diffraction and reflection at inlets*. Coastal Inlets Research Program, ERDC/CHL CHETN-III-73. Vicksburg, MS: U.S. Army Engineer Research and Development Center. An electronic copy of this CHETN is available from <http://chl.erdc.usace.army.mil/chetn>.

REFERENCES

- Cartwright, D. E. 1963. The use of directional spectra in studying output of a wave recorder on a moving ship, *Ocean Wave Spectra: Proceedings of a Conference*, Prentice-Hall, Inc., 203-218, Englewood Cliffs, NJ.
- Holthuijsen, L. H., A. Herman, and N. Booij. 2004. Phase-decoupled refraction-diffraction for spectral wave models. *Coastal Engineering* 49, 291-305.
- Isobe, M. 1998. Equation for numerical modeling of wave transformation in shallow water. Wave phenomena and offshore topics. Chapter 3 in *Developments in offshore engineering*, J. B. Herbich, ed., 101-162, Houston, TX: Gulf Publishing Co.
- Lin, L., and Z. Demirbilek. 2005. Evaluation of two numerical wave models with inlet physical model. *Journal of Waterway, Port, Coastal, and Ocean Engineering* 131(4), 149-161.
- Longuet-Higgins, M. S., and R. W. Stewart. 1964. Radiation stresses in water waves: A physical discussion with applications. *Deep-Sea Research* 11, 529-562.
- Mase, H. 2001. Multi-directional random wave transformation model based on energy balance equation. *Coastal Engineering Journal* 43(4), 317-337.
- Mase, H., and T. Kitano. 2000. Spectrum-based prediction model for random wave transformation over arbitrary bottom topography. *Coastal Engineering Journal* 42(1), 111-151.

- Mase, H., K. Oki, T. Hedges, and H. J. Li. 2005. Extended energy-balance-equation wave model for multi-directional random wave transformation. *Ocean Engineering* 32, 961-985.
- Militello, A., C. W. Reed, A. K. Zundel, and N. C. Kraus. 2004. *Two-dimensional depth-averaged circulation model M2D: Version 2.0, Report 1: Technical documentation and user's guide*. Coastal Inlets Research Program, Technical Report ERDC/CHL TR-04-2, Vicksburg, MS: U.S. Army Engineer Research and Development Center.
- Panchang, V., and Z. Demirbilek. 1998. Wave prediction models for coastal engineering applications. Wave phenomena and offshore topics. Chapter 4 in *Developments in offshore engineering*, J. B. Herbich, ed., 163-194, Houston, TX: Gulf Publishing Co.
- Penney, W. G., and A. T. Price. 1952. The diffraction theory of sea waves by breakwaters and shelter afforded by breakwaters. *Philos. Trans. Roy. Soc. London Ser. A*, 244, 236-253.
- Rivero, F. J., A. S. Arcilla, and E. Carci. 1997a. Implementation of diffraction effects in the wave energy conservation equation. *IMA Conference On Wind-Over-waves Couplings: Perspectives and Prospects*, The University of Salford, UK.
- Rivero, F. J., A. S. Arcilla, and E. Carci. 1997b. An analysis of diffraction in spectral wave models. *Proceedings 3rd International Symposium of Ocean Wave Measurement and Analysis, Waves '97*, ASCE, 431-445.
- Seabergh, W. C., W. R. Curtis, L. J. Thomas, and K. K. Hathaway. 2002. *Physical model study of wave diffraction-refraction at an idealized inlet*. Coastal Inlets Research Program, Technical Report ERDC/CHL-TR-02-27, Vicksburg, MS: U.S. Army Engineer Research and Development Center.
- Seabergh, W. C., L. Lin, and Z. Demirbilek. 2005. *Laboratory study of hydrodynamics near absorbing and fully reflecting jetties*. Coastal Inlets Research Program, Technical Report ERDC/CHL-TR-05-8, Vicksburg, MS: U.S. Army Engineer Research and Development Center.
- Smith, J. M., D. T. Resio, and A. Zundel. 1999. *STWAVE: Steady-state spectral wave model, Report 1: User's manual for STWAVE version 2.0*. Instruction Report CHL-99-1, Vicksburg, MS: U.S. Army Engineer Waterways Experiment Station.
- Yu, Y.-X., S.-X. Liu, Y. S. Li, and O. W. H. Wai. 2000. Refraction and diffraction of random waves through breakwater. *Ocean Engineering* 27, 489-509.

NOTE: The contents of this technical note are not to be used for advertising, publication, or promotional purposes. Citation of trade names does not constitute an official endorsement or approval of the use of such products.